

Water Jet Propulsion Mechanism for Low Speed AUV

A. Suzuki*, H. Kondo* and M. Osakabe*

* Graduate School of Marine System Engineering, Tokyo University of Marine Science and Technology, 2-1-6 Etchujima, Koto-ku, Tokyo 135-8533, Japan

Autonomous Underwater Vehicle (AUV) propelled with pump jet injection system was proposed. The propulsion mechanism has special duct wings surrounding the AUV body and the seawater is injected into the space between the wings and body with the nozzles. The high speed pump jet can be converted to the low speed and high mass jet by sucking the peripheral seawater. The nozzles use Coanda effect to stay the injected jet on the AUV body surface side. The water injection behavior from the Coanda nozzles between the AUV body and the duct wings was studied in a simple rectangular duct. The injected jet velocity and angle affected the suction flow rate and the mixing behavior. When the jet flows stayed on the surface due to the Coanda effect, the suction flow rate was generally increased. On the other hands, when the jet flow was separated from the surface, the suction flow rate was significantly reduced. The mixing flow pattern around the nozzle was also studied with the three-dimensional numerical simulation code with the turbulence model. The predictions generally agreed well with the experimental results but the further improvement was pointed out.

Keywords: AUV, Pump jet, Suction flow, Propulsion, Coanda effect

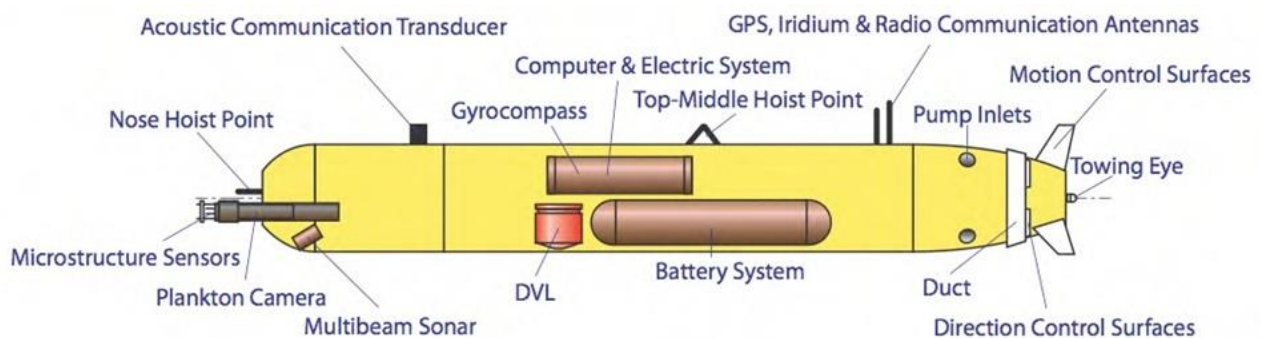


Fig. 1 Schematics of AUV without propeller

1. Introduction

Almost all the Autonomous Underwater Vehicle (AUV) gets the propulsion force with the propeller. However, the propeller has a possibility to be entangled with seaweeds and the emitting noises affect the sophisticated sensors on AUV to observe the peripheral circumstance. Therefore, AUV propelled with pump jet injection system was proposed to minimize these problems^[1]. The high speed and low noise pump is used for the propulsion. However, the pump jet injection system is less efficient than the propeller, especially at a low speed

of AUV.

To increase the efficiency at low speed, the high speed pump jet should be converted to the low speed and high mass jet by sucking the peripheral seawater. To increase the suction flow, the propulsion mechanism has special duct wings surrounding the AUV body and the seawater is injected into the space between the wings and body with the nozzles. The nozzles use Coanda effect to stay the injected jet on the AUV body surface side. The surface jet can efficiently introduce the peripheral seawater into the space between the wings and body. The low speed and high mass jet

released from the space can propel the AUV efficiently even at a low cruising velocity.

The water injection behavior from the Coanda nozzles between the AUV body and the duct wings was studied in a simple rectangular duct. The mixing flow pattern around the nozzle was also studied with the three-dimensional numerical simulation code with the low-Reynolds $k-\epsilon$ turbulence model.

2. AUV without propeller

2.1 Schematics of AUV

Although the vehicle's cruising speed is slow, the vehicle's size should be longer than 3 meters. The Microstructure sensors and the plankton camera should be mounted on the nose of the vehicle to measure at a point where the vehicle's wake doesn't disturb it. Figure 1 shows a general arrangement of the designed cruising-style AUV. The AUV has a torpedo-like shape, which diameter is 0.6m.

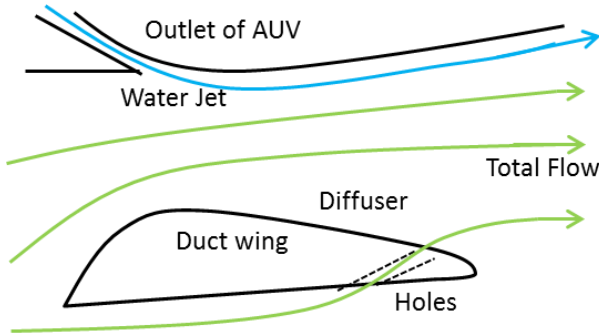


Fig. 2 Injection port of propulsion system

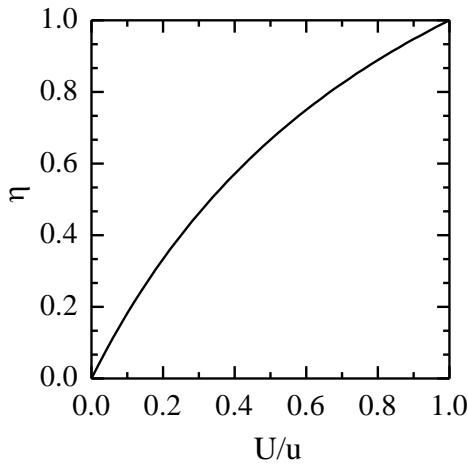


Fig. 3 Jet propulsion efficiency

The length is about 4.5m and it can be separated into 3 parts for easy transportation which can be divided into the head for the measuring system, the middle for computer and battery systems, and the tail for propulsion and motion control systems.

As shown in Fig.2, the propulsion mechanism has special duct wings surrounding the AUV body. The seawater is injected with the high speed and low noise pump and the surface jet can efficiently introduce the peripheral seawater into the space between the wings and body.

2.2 Efficiency

The propulsion thrust force of AUV is

$$F = G(u - U) \quad (1)$$

where G is the discharging mass, u the discharging velocity, and U the cruising velocity of AUV. The jet propulsion efficiency η is defined as the ratio of thrust work and the kinetic energy provided by the AUV.

$$\eta = \frac{FU}{\frac{1}{2}G(u^2 - U^2)} \quad (2)$$

By using Eq.(1), the above equation can be simply expressed as

$$\eta = \frac{2\frac{U}{u}}{\left(1 + \frac{U}{u}\right)} \quad (3)$$

Shown in Fig.3 is the propulsion efficiency calculated with Eq.(3). The propulsion efficiency is large when the AUV cruising velocity U and the discharging velocity u is approximately the same. The velocity ratio U/u should be large to increase the propulsion efficiency. When the cruising velocity is given, the reduction of discharging velocity is necessary.

The discharging mass is the sum of pump mass flow rate and suction mass flow rate as,

$$G = G_{Pump} + G_{Suc} \quad (4)$$

The suction flow ratio is defined as,

$$\phi = \frac{G_{Suc}}{G_{Pump}} \quad (5)$$

For the reduction of discharging velocity, the increase of the suction flow rate is necessary.

When the kinetic energy supplied by pump is converted to the discharging energy without any loss,

$$\frac{1}{2}G_{Pump}u_{Pump}^2 = \frac{1}{2}Gu^2 - \frac{1}{2}G_{Suc}U^2 \quad (6)$$

Substituting the above equation into Eq.(2),

$$\eta = \frac{FU}{\frac{1}{2}G_{Pump}(u_{Pump}^2 - U^2)} \quad (7)$$

The jet propulsion efficiency η is also expressed as the ratio of thrust work and the kinetic energy provided by the pump.

3. Experiment

3.1 Experimental method

The water injection behavior from the Coanda nozzles between the AUV body and the duct wings was studied in a simple rectangular duct (width: 50mm, height: 20mm, length: 514mm) as shown in Fig.4. The nozzles of 6 different types are prepared. The nozzle is the two-dimensional curved channel to use Coanda effect^[2]. The fluid tends to flow on the curved surface without the separation. The centrifugal force makes the lower pressure on the curved surface and prevents the separation of fluid jet from the surface.

The injection nozzle plate as the duct upper surface is shown in Fig.5. The thickness of nozzle plate is 30mm. The inner radius R is 5mm, 10mm or 15mm. The tangential direction of the inner radius coincides with the nozzle plate bottom line. The nozzle width is 2mm or 5mm. These values determine the nozzle injection angle θ of the outer radius as,

$$\cos \theta = \frac{R}{R+W} \quad (8)$$

The 6 nozzles as indicated in Table 1 can be installed in the test section. Although AUV is in open flow system, to obtain the value of flow rate, the test section is connected to 2 tanks which are also connected by another large pipe called as the circulation line. Water level in the both tanks is

maintained at the same with the circulation line. The suction flow has the loss due to the circulation in the pipe system, and its value is smaller than in the open flow. The tanks are exposed to the atmosphere on their ceiling.

The water from tank2 is injected to the test section by the Ebara line pump (LPD type) after measuring the flow rate. The vortex flow meter, Tokyo Keiso VF-2000 (range 4-40 L/min., error $\pm 3\%$ F.S.) is used for the injected pump flow. For the suction flow to the test section, the electromagnetic flow meter, Tokyo Keiso MAGMAX EGM4100C (error $\pm 0.5\%$, ± 0.01 mA) is used.

The steady flow rates are during 30 second after five minutes of initial pump running.

Table 1 Nozzles for experiment

nozzle name	R5W2	R10W2	R15W2
R mm	5	10	15
W mm	2	2	2
θ degree	44.42	33.56	28.07

nozzle name	R5W5	R10W5	R15W5
R mm	5	10	15
W mm	5	5	5
θ degree	60.00	48.19	41.41

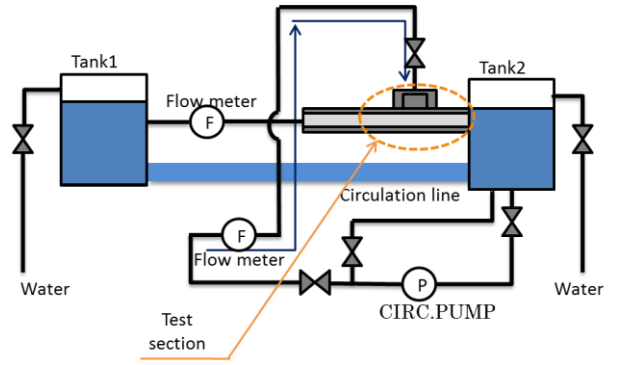


Fig.4 Experimental apparatus

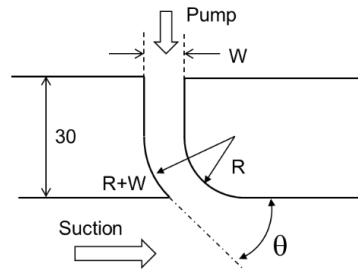


Fig. 5 Injection nozzle plate

3.2 Result and discussion

Shown in Fig.6 is the relation of pump and suction flow rate. The suction flow rate increases as the increase of pump flow rate. The suction flow rate strongly depends on the nozzle shape. The vertical axis is changed to suction ratio ϕ in Fig.7. The largest suction ratio is obtained at R10w2, followed in order by R15w2, R5w2, R15w5, R10w5, and R5w5. Their ratios ϕ are almost constant. The suction flow rate is indicated as 0 kg/s with R5w5 less than the pump flow rate of 0.06 kg/s. In this range, the reverse flow is observed.

The smaller nozzle width results as the larger ratio. At the same pump mass flow rate, the smaller width results as the higher injection velocity and the higher suction flow rate. When the width is 5mm, the suction ratio is proportional to the radius. However, the ratio is not proportional to the radius at the width of 2mm.

Generally, the larger radius results as the smaller injection angle as shown in Table 1 and the injected flow tends to stay on the upper duct surface as shown in the experimental result for the width of 5mm. However, the larger radius reduces the centrifugal force and increases the surface pressure to enhance the separation. In the width of 2mm, the suction ratio for the radius of 10mm becomes larger than that for the radius of 15mm.

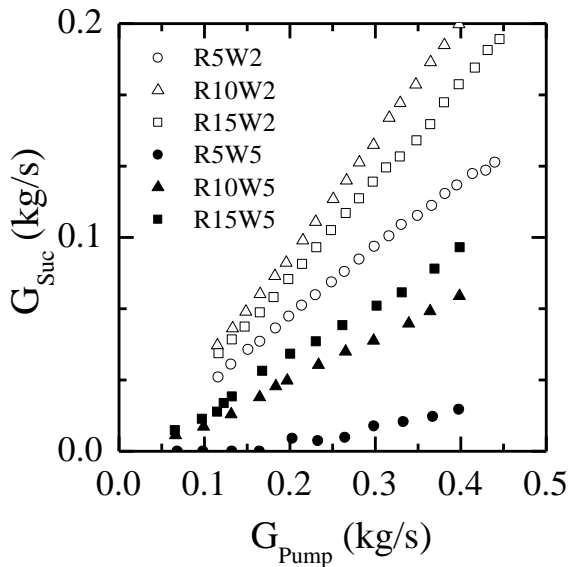


Fig. 6 Relation of pump and suction flow rate

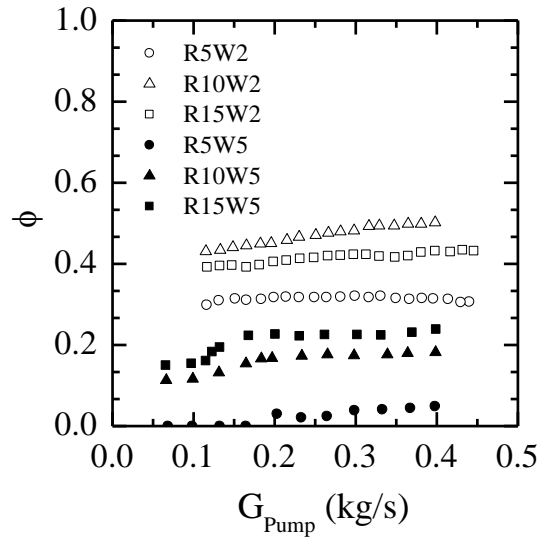


Fig. 7 Relation of suction ratio and pump flow rate

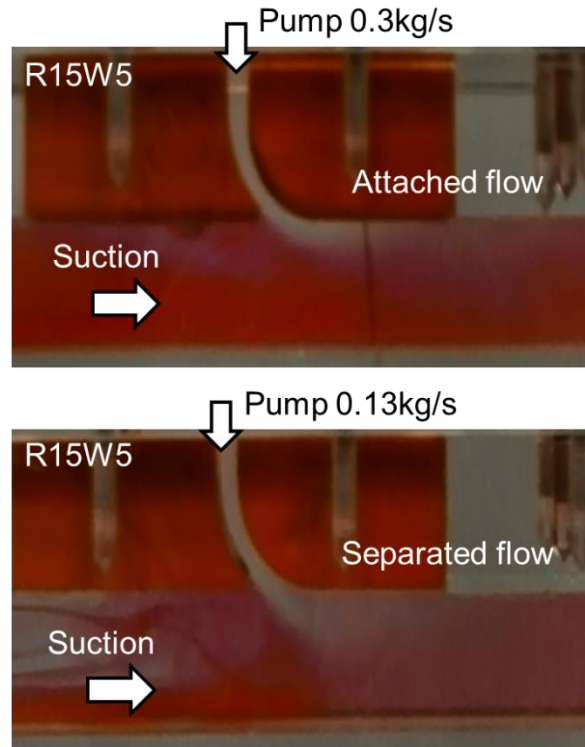


Fig. 8 Injection behavior of R15W5 nozzle

Some nozzles cause the injection flow which separated from the upper side surface of the test duct. Shown in Fig.8 is the attached and separated flow observed in R15W5 nozzle. The pump flow is injected into the suction flow colored with a red ink. It should be noted that the higher injection prevents the separation. The separated flow is observed with R5w2, R5w5 and R10w5 in the all experimental range of this study. The separated flow with R15w5

is observed only at the pump flow rate less than 0.13 kg/s.

According to the above result, the flow which attached on the upper side of the test section surface is more efficient to increase the suction ratio than the separated flow.

Shown in Fig.9 is the relation of suction ratio and injection angle at the pump flow rate of 0.4kg/s in the 6 nozzles. As the decrease of injection angle with the larger radius and the smaller width, the separated flow changes to the attached flow and the suction ratio increases. However, the larger radius reduces the centrifugal force and increases the surface pressure. The lower surface pressure is expected to make the stable surface jet to introduce the larger suction flow. So the suction ratio is not simply proportional to the injection angle.

4. Simulation

4.1 Simulation code

The three-dimensional numerical simulation code “SOLIDWORKS” was used for the present prediction. The low-Reynolds $k-\epsilon$ turbulence model is used in the code. The experimental equipment including the tanks was modeled on 3D CAD^[3], though the pump is defined just as the boundary conditions and the free water surface in tanks are not modeled. The calculation mesh was enough small to obtain the precise predictions.

4.2 Result and Discussion

Shown in Fig.10 is the 3D stream lines observed

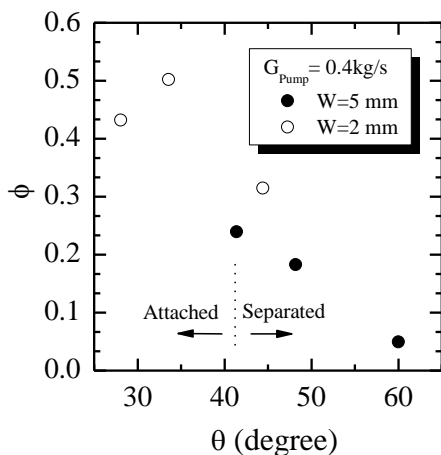


Fig. 9 Relation of suction ratio and injection angle

from the duct side in R5W2 nozzle indicating the separated flow. Injected flow penetrates to the bottom of the test duct. The suction flow is blocked by the penetrating jet. The experimental results show the reduction of suction flow at the separated flow and the calculation results also support the reduction. Shown in Fig.11 is the 3D stream lines in R10w2 nozzle indicating the attached flow on the upper surface of test duct. Injected flow smoothly introduces the suction flow from the left.

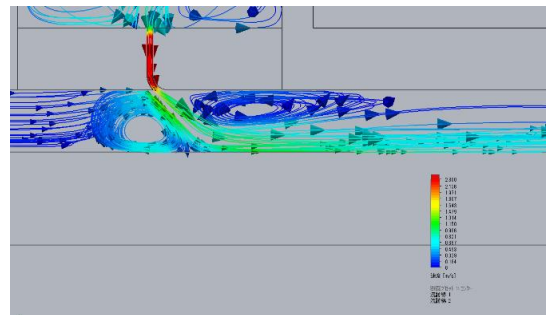


Fig. 10 Separated flow in R5W2 nozzle

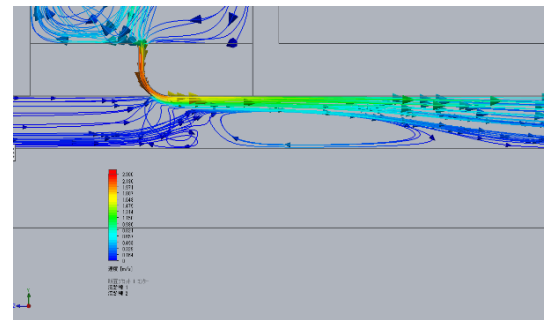


Fig11. Attached flow in R10W2 nozzle

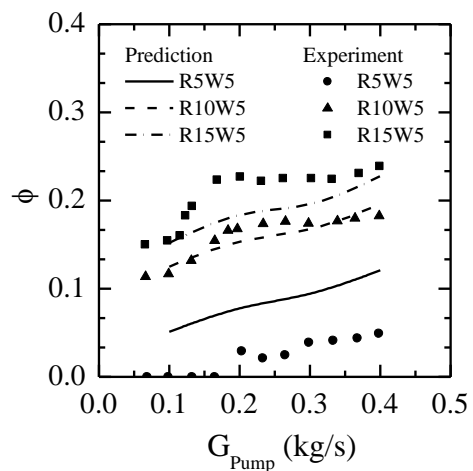


Fig12. Comparison of calculation and experimental data in width 5mm nozzle

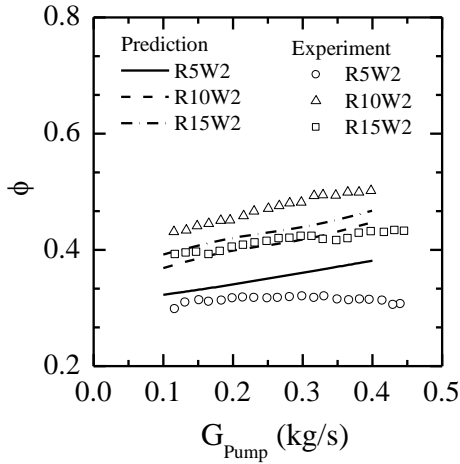


Fig13. Comparison of calculation and experimental data in width 2mm nozzle

Shown in Fig12 is the comparison of calculation and experimental data in the nozzle of width 5mm. The larger radius results as the larger suction ratio in the prediction as same as the experimental results. The prediction is not good for the radius of 5 and 15mm but agree well for the radius of 10mm.

Shown in Fig13 is the comparison of calculation and experimental data in the nozzle of width 2mm. The larger radius results as the larger suction ratio in the prediction but the experimental results have a maximum suction ratio at the radius of 10mm. The prediction generally agrees well with the experimental results but the further improvement is necessary.

5. Conclusion

AUV propelled with pump jet injection system was proposed. The water injection behavior from the Coanda nozzles between the AUV body and duct wing was studied in a simple rectangular duct. The followings are major results obtained in the present experiment and simulation.

1. The smaller nozzle width results as the larger suction ratio at the same pump mass flow rate. When the nozzle width is 5mm, the suction ratio is proportional to the nozzle radius. However, the ratio is not proportional to the radius at the width of 2mm.
2. Generally, the larger radius and the smaller width results as the smaller injection angle, and the injected flow tends to stay on the upper

duct surface. On the other hand, the larger radius reduces the centrifugal force and increases the surface pressure. The lower surface pressure is expected to make the stable surface jet to introduce the larger suction flow. So the suction ratio is not simply proportional to the radius at the width of 2mm.

3. The larger radius results as the larger suction ratio in the prediction but the experimental results sometimes have a maximum suction ratio. The predictions generally agree well with the experimental results but the further improvement is necessary.

Acknowledgment

This work was supported by JST CREST Grant Number JPMJCR12A6, Japan.

References

- [1] Kondo, H., Sato, M., Hotta, T., Withamana, A., Osakabe, M. and Matsumoto, Y. Development of a Marine Ecosystem and Microstructure Monitoring AUV for Plankton Environment, Proc. of IEEE AUV 2014, (2014).
- [2] Coanda, H., "PROPELLING DEVICE," US Patent 2108652, Feb. 15, 1938, Filed Jan. 10, 1936.
- [3] 3D CAD Design Software SLIDWORKS, <http://www.solidworks.com> (accessed on 15 April, 2017).

Nomenclature

G : mass flow rate [kg/s]
 R : radius [mm]
 u : discharging velocity [m/s]
 U : cruising velocity [m/s]
 w : width [mm]
 ϕ : suction ratio [-]
 η : efficiency [-]
 θ : jet injection angle [degree]

Subscript

Pump: pump

Suc: suction